

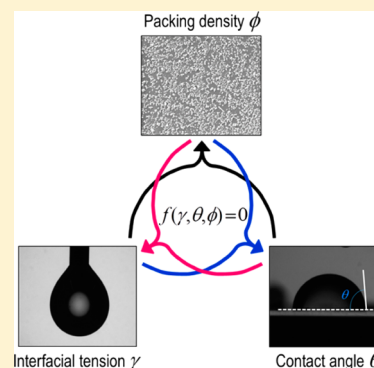
# Interfacial Activity of Nonamphiphilic Particles in Fluid–Fluid Interfaces

Yi Zhang, Songcheng Wang, Jiarun Zhou, Ruiyang Zhao,<sup>1</sup> Gregory Benz, Stephane Tcheimou, J. Carson Meredith,<sup>2\*</sup> and Sven H. Behrens<sup>3\*</sup>

School of Chemical & Biomolecular Engineering, Georgia Institute of Technology, Atlanta, Georgia 30332-0100, United States

## Supporting Information

**ABSTRACT:** Surfactants can adsorb in fluid–fluid interfaces and lower the interfacial tension. Like surfactants, particles with appropriate wettability can also adsorb in fluid–fluid interfaces. Despite many studies of particle adsorption at fluid interfaces, some confusion persists regarding the ability of (simple, nonamphiphilic) particles to reduce the interfacial tension. In the present work, the interfacial activity of silica nanoparticles at air–water and hexadecane–water interfaces and of ethyl cellulose particles at the interface of water with trimethylolpropane trimethacrylate was analyzed through pendant drop tensiometry. Our measurements strongly suggest that the particles do significantly affect the interfacial tension provided that they have a strong affinity to the interface by virtue of their wettability and that no energy barrier to adsorption prevents them from reaching the interface. A simplistic model that does not explicitly account for any particle–particle interactions is found to yield surprisingly good predictions for the effective interfacial tension in the presence of the adsorbed particles. We further propose that interfacial tension measurements, when combined with information about the particles' wetting properties, can provide a convenient way to estimate the packing density of particles in fluid–fluid interfaces. These results may help to understand and control the assembly of nonamphiphilic nanoparticles at fluid–fluid interfaces, which is relevant to applications ranging from surfactant-free formulations and food technology to oil recovery.



## INTRODUCTION

Surfactants and amphiphilic macromolecules tend to adsorb in fluid–fluid interfaces and lower the interfacial tension. The interfacial adsorption of surfactants can also provide a steric or electrostatic barrier to the coalescence of liquid droplets or of gas bubbles. In addition to stabilizing emulsions and foams, they act as wetting modifiers (wetting agents) in many products such as detergents for laundry and dish washing, coatings, or pharmaceutical formulations.<sup>1</sup> Like surfactants, particles with appropriate wettability can also adsorb to fluid–fluid interfaces; in fact, they typically adsorb more strongly.<sup>2,3</sup> The energy required to remove a particle from the interface by transferring it to the nearest fluid bulk is given by<sup>4,5</sup>

$$\Delta E = -\pi R^2 \gamma_{ij} (1 - |\cos \theta_{ij}|)^2 \quad (1)$$

where  $\gamma_{ij}$  denotes the surface (interfacial) tension,  $\theta_{ij}$  is the contact angle of a single particle at the interface, and  $R$  is the particle radius. For particles in the colloidal size range, this energy can easily exceed the thermal energy by orders of magnitude and thus making particle attachment to the interface practically irreversible.

As a result of this strong attachment, adsorbed particles can inhibit bubble or droplet coalescence and coarsening. Since the pioneering work of Ramsden and Pickering in the early 20th century,<sup>6,7</sup> numerous studies on using particles as stabilizers in the interface have been conducted. Particle-stabilized foams<sup>8</sup>

and emulsions<sup>9–11</sup> have been studied in a variety of fields ranging from materials science to catalysis and from food science to biomedicine and the use of chemical sensors. In addition to foams and emulsions, new classes of soft materials, such as bijels,<sup>12</sup> colloidosomes,<sup>13</sup> liquid marbles,<sup>14,15</sup> and capillary foams,<sup>16,17</sup> have also been prepared using particles as stabilizers.

Despite many studies about the adsorption of particles in the interface, there appears to be no general consensus on whether simple, nonamphiphilic particles adsorbed at an interface will reduce the interfacial tension. Some studies show that often particles do not do so,<sup>18–24</sup> but other studies suggest that they can,<sup>25–31</sup> as summarized in Table 1. Vignati et al. demonstrated that the adsorption of silanized silica particles at the water–isooctane interface did not lead to appreciable changes in droplet interfacial tension.<sup>19</sup> Fernandez-Rodriguez et al. reported that functionalized silica particles and homogeneous poly(methyl methacrylate) particles did not strongly reduce the water–decane interfacial tension.<sup>20</sup> Moghadamis et al. demonstrated that the presence of ZnO nanoparticles had no significant effect on the *n*-decane–water interfacial tension.<sup>21</sup> Pichot et al. observed no effect of hydrophilic silica particles on the vegetable oil–water interfacial tension.<sup>22</sup> Drelich et al.

Received: February 21, 2017

Revised: April 12, 2017

Published: April 19, 2017

**Table 1. Summary of Recent Work on the Effect of Particle Adsorption on the Interfacial Tension**

| particle  | type of interface  | change of interfacial tension   | ref                                      |
|---|--|---------------------------------|--|
| silanized silica particles                          | water–isooctane  | no obvious change               | Vignati et al. <sup>19</sup>             |
| functionalized silica particles                     | water–decane   | no obvious change               | Fernandez-Rodriguez et al. <sup>20</sup> |
| homogeneous poly(methyl methacrylate) particles     | water–decane   | no obvious change               | Fernandez-Rodriguez et al. <sup>20</sup> |
| ZnO   | <i>n</i> -decane–water   | no obvious change               | Moghadamis et al. <sup>21</sup>          |
| hydrophilic silica particles                        | vegetable oil–water  | no obvious change               | Pichot et al. <sup>22</sup>              |
| hydrophobic silica particles                        | paraffin oil–water   | no obvious change               | Drelich et al. <sup>23</sup>             |
| sterically stabilized pH responsive latex particles | hexadecane–water (pH = 2)                                      | no obvious change               | Manga et al. <sup>24</sup>               |
| charge-stabilized titania                           | air–water  | significant decrease            | Dong et al. <sup>25</sup>                |
| ethyl cellulose particles                           | air–water  | decrease from 72.3 to 38.9 mN/m | Bizmark et al. <sup>26</sup>             |
| partially hydrophobic fumed silica particles        | air–water  | decrease from 72.8 to 50.0 mN/m | Stocco et al. <sup>27</sup>              |
| Au-cit or Au-TEG nanoparticles                      | octafluoropentyl acrylate (OFPA)–water                         | slight decrease                 | Du et al. <sup>28</sup>                  |
| Au-TEG or PS particles                              | fluorohexane–water   | slight decrease                 | Du et al. <sup>28</sup>                  |
| carboxyl-terminated carbon black (CB) particles     | <i>n</i> -dodecene–water                                       | decrease from 30 to 8.5 mN/m    | Powell et al. <sup>29</sup>              |
| gold nanoparticles                                  | toluene–water  | decrease from 23.2 to 9.7 mN/m  | Hua et al. <sup>30</sup>                 |
| cellulosic particles                                | air–water and triethylene glycol dimethacrylate (TEGDMA)–water | significant decrease            | Zhang et al. <sup>31</sup>               |

showed that no interfacial tension reduction was observed at the paraffin oil–water interface in the presence of hydrophobic silica particles.<sup>23</sup> Manga et al. found that charge-stabilized particles had little or no influence on the interfacial tensions.<sup>24</sup> Other studies demonstrated that particles *can* lower the interfacial tensions.<sup>25–31</sup> Dong et al. showed that the surface tension of charge-stabilized titania suspensions first decreased significantly and then increased to a plateau with the increase of particle concentration.<sup>25</sup> Bizmark et al. reported that the adsorption of ethyl cellulose particles lowered the surface tension of air–water interface from 72.3 to 38.9 mN/m.<sup>26</sup> Stocco et al. demonstrated that partially hydrophobic fumed silica particles could reduce the air–water surface tension value from 72.8 to around 50 mN/m.<sup>27</sup> Du et al. showed that the adsorption of Au-cit or Au-TEG nanoparticles to the octafluoropentyl acrylate (OFPA)–water interface and the adsorption of Au-TEG or PS particles to the fluorohexane–water interface all slightly lowered the interfacial tension.<sup>28</sup> Powell et al. reported that carboxyl-terminated carbon black (CB) particles could decrease the *n*-dodecene–water interfacial tension from 30 to 8.5 mN/m.<sup>29</sup> Hua et al. found that gold nanoparticles could lower the toluene–water interfacial tension from 23.2 to 9.7 mN/m.<sup>30</sup> In an earlier study, we found that cellulosic particles can be used to change both air–water surface tension and oil–water interfacial tension.<sup>31</sup> When a significant interfacial tension reduction is observed, the effect is generally explained by a large adsorption energy of particles at the interface. When no change in interfacial tension is observed, the results are often declared “not surface active” even though adsorption is believed to take place.<sup>32</sup>

In this paper, we present a systematic study of interfacial tension effects caused by silica particles with different hydrophobicity. Our results suggest that these particles can change the interfacial tension as long as they have sufficiently strong affinity for the interface and do make physical contact with it. A simple model that does not explicitly account for any particle–particle interaction is seen to predict surprisingly well the effective interfacial tension due to the adsorption of particles in the fluid–fluid interfaces. Finally, this study

provides a convenient way to estimate the packing density of particles in fluid–fluid interfaces by combining dynamic interfacial tension measurements with information about the particles’ wetting properties.

## ■ MATERIALS AND METHODS

**Materials.** Wacker-Chemie AG provided fumed silica particles in powder form with different degrees of hydrophobicity: HDK N20 (unmodified, 100% SiOH coverage) and MM038-5 (68% methylsilyl capped, 32% SiOH). Methylsilyl modification was performed by the manufacturer through reaction with dichlorodimethylsilane.<sup>33</sup> Direct measurement of the particle contact angle, for example, by the gel trapping method,<sup>34</sup> freeze-fracture shadow-casting cryo-scanning electron microscopy (FreSCa cryo-SEM),<sup>35</sup> or digital holography,<sup>36</sup> is a challenging task for small particles of fumed silica with nonspherical shapes. The wettability of silica particles was assessed in an approximate fashion by measuring the contact angle of a water drop in air on a pressed tablet of silica particles. The particles’ hydrodynamic radius in water was measured by dynamic light scattering using a Malvern Zetasizer Nano ZS90. The hydrodynamic radius and wettability of silica particles are shown in Table 2.

**Table 2. Hydrodynamic Radius and Wettability of Silica Particles with and without Surface Modification. Contact Angle Data of 100% SiOH Silica Particles Were Obtained from the Literature<sup>37</sup>**

| particle (residual silanol) | surface modification | particle hydrodynamic radius (nm) in water | contact angle at air–water interface (deg) |
|-----------------------------|----------------------|--|--|
| 100% SiOH                   | none                 | 252 ± 19                                   | 20 ± 5                                     |
| 32% SiOH                    | 68% methylsilyl      | 239 ± 22                                   | 114 ± 9                                    |

Trimethylolpropane trimethacrylate (TMPTMA) and *n*-hexadecane were bought from Sigma-Aldrich. TMPTMA was treated with Al<sub>2</sub>O<sub>3</sub> to remove an inhibitor present in the purchased monomer and was enriched with 6 wt % of the photoinitiator benzoin isobutyl ether for experiments requiring polymerization. The *n*-hexadecane was purified by mixing it with basic alumina and silica gel, allowing it to stand overnight, and then separating it through centrifugation. Ultrapure water with a resistivity of 18.2 MΩ·cm (Barnstead) was used. Since the

partially hydrophobic silica particles (32% SiOH) do not disperse easily in DI water, aqueous dispersions were prepared by first dispersing the particles in acetone and then transferring them to the DI water using repeated centrifugation and replacement of the supernatant.

**Synthesis and Characterization of Ethyl Cellulose Nanoparticles.** Ethyl cellulose (EC) particles were synthesized by following the reported method.<sup>38</sup> Briefly, a 1 wt % solution of EC (Sigma-Aldrich, product code: 247499-100G) in acetone was prepared using a magnetic stirrer at 1100 rpm and 45 °C until the EC was dissolved. An equal volume of ultrapure DI water was then quickly poured into the EC solution while stirring it at 1100 rpm, after which the solution became turbid as a result of EC nanoparticles' nucleation and growth. Then the acetone and part of the water were removed by evaporation, and the EC particle suspension was purified by passing it three times through a C18–silica chromatographic column (Phenomenex) that had been preactivated with an acetonitrile–water (80:20) mixture and flushed several times with hot DI water. The hydrodynamic radius of the EC particles in the presence of 50 mM NaCl was measured through dynamic light scattering using a Malvern Zetasizer Nano ZS90. The diameter of the EC particles inferred from the z-average of the diffusion coefficient is  $102 \pm 13$  nm. The contact angle of EC particles in the TMPTMA–water interface was also measured. The detailed procedure and result are presented in the following sections.

**Tensiometry.** The dynamic interfacial tension was measured via axisymmetric drop shape analysis using a Ramé-hart goniometer (model-250). This method has been widely used for determining the evolution of the interfacial tension due to the adsorption of particles to the interface. Briefly, a pendant droplet was created by a syringe with a steel needle, and a CCD camera was programmed to capture the variation of drop shape over time. The interfacial tension was obtained by analyzing the contour shape resulting from the balance of gravitational forces and tension forces. All experiments were performed at a room temperature of 21 °C. The dynamic and long-term interfacial tensions for air–water and oil–water in the absence and presence of particles were measured at different particle concentrations. In all our measurements, the interfacial tension has reached steady state and remained constant after 1800 s, so we took the value at  $t = 1800$  s as the long-term interfacial tension.

**Contact Angle.** Prior to the experiment, a TMPTMA phase and a water phase were mutually saturated by vigorously mixing equal liquid volumes overnight and separating them with centrifugation until phase separation was achieved. The contact angle of EC particles in the TMPTMA–water interface was investigated using a Ramé-Hart goniometer and a TMPTMA droplet in water on a proxy surface mimicking the EC particles. An EC-coated substrate was prepared from particles dissolved in acetone using spin coating (1000 rpm, 60 s). The measurements were carried out in a quartz cell filled with water. The substrate was submerged in the quartz cell and suspended by a holder. A drop of TMPTMA, which is slightly denser than water, was then deposited on the substrate with a 22 gauge needle.

**Packing Density.** The packing density ( $\phi$ ) of EC particles in the TMPTMA–water interface was measured by analyzing scanning electron microscopy (SEM) images of particles trapped in a polymerized TMPTMA droplet. Briefly, a droplet of TMPTMA immersed in an EC particles suspension was created by a syringe with a steel needle. After the EC particles adsorbed to the interface (at  $t = 1800$  s, this time scale is selected based on the dynamic surface tension measurement result in which the surface tension shows steady state at 1800 s), the TMPTMA droplet was polymerized using a UV lamp. The cured TMPTMA droplets with EC particles in the interface were sputter-coated with a thin layer of gold, and SEM images were taken using a Zeiss Ultra60 field emission scanning electron microscope (FE-SEM; Carl Zeiss Microscopy, LLC North America, Peabody, MA).

## RESULTS AND DISCUSSION

**Effect of Silica Particles on Water Surface Tension.** To study the influence of simple, nonamphiphilic particles on the surface tension of water, the surface tension of 1 wt %

hydrophilic silica particle (100% SiOH) suspension was measured by pendant drop shape analysis using a Ramé-hart tensiometer. Figure 1a shows that the surface tension remains

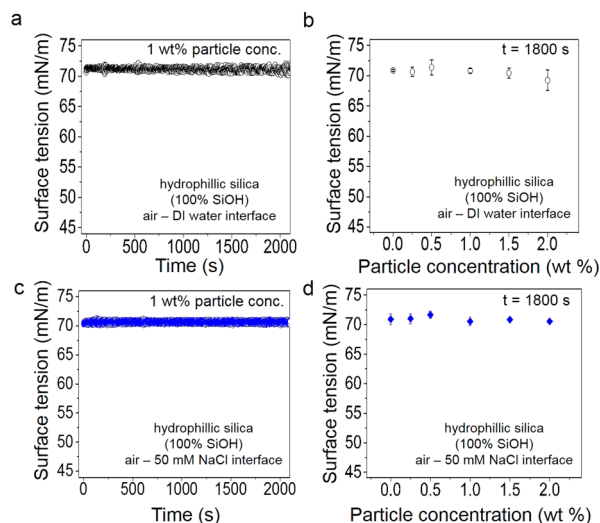


**Figure 1.** Interfacial activity of hydrophilic silica particles (100% SiOH) in the air–water interface. (a) Surface tension over time for 1 wt % particle dispersion. (b) Steady state surface tension obtained at  $t = 1800$  s for various particle concentrations. (c) Surface tension over time for 1 wt % particle dispersion in the presence of 50 mM NaCl. (d) Steady state surface tension obtained at  $t = 1800$  s for various concentrations of the surface-modified silica particles in the presence of 50 mM NaCl. Error bars represent the standard deviation of at least three replicate measurements.

unchanged over time. In addition, we determined the dependence of the surface tension (taken at  $t = 1800$  s) on particle concentrations ranging from 0 to 2 wt %. Figure 1b shows some scatter in the surface tension measured for different particle concentrations, but in general, the surface tension of hydrophilic silica particle suspensions remained within  $\pm 1$  mN/m of the value for particle-free deionized water. Figure 1b demonstrates that hydrophilic silica particles do not significantly reduce the tension of the air–water interface. We first suppose that an energy barrier to particle adsorption may limit the interfacial activity of hydrophilic silica particles. It is well-known that both silica particles in water and a bare air–water interface tend to carry an electric surface charge due to dissociable surface groups in the case of silica<sup>39</sup> and due to ion adsorption in the case of the air–water interface.<sup>40–42</sup> As a result, an electrostatic barrier can hinder the particle adsorption at the air–water interface<sup>26,43,44</sup> in a similar way that electrostatic barriers can hinder particle adsorption to oil–water interfaces.<sup>45–47</sup> For particles near an air–water interface, repulsive London–van der Waals interaction with the interface also oppose particle adsorption.<sup>48</sup> The electrostatic interaction between particles and the interface can be screened by salt ions. To test our hypothesis, we measured the dynamic surface tension of a 1 wt % dispersion of the same hydrophilic silica particles (100% SiOH) containing 50 mM NaCl. Figures 1c and 1d demonstrate that hydrophilic silica particles do not show significant interfacial activity even in the presence of salt. We then believe that 100% SiOH silica particles are too hydrophilic to adsorb strongly at the air–water interface (the contact angle with the air–water interface is  $20 \pm 5^\circ$ ).<sup>49</sup> Okubo et al. tested the effects of colloidal particles on the equilibrium

air–water surface tension and also found that hydrophilic colloidal silica can increase or decrease the equilibrium surface tension at the air–water interface only slightly.<sup>50</sup>

Expecting that hydrophobically modified silica particles with a strong affinity to the air–water interface can substantially reduce the surface tension, we turn to a system containing the more hydrophobic silica particles (32% SiOH), which can strongly adsorb on the air–water interface and are known to be good stabilizers for aqueous foams.<sup>51</sup> We measured the dynamic surface tension of 1 wt % particle dispersion over time as particles adsorbed at the interface (Figure 2a). We also

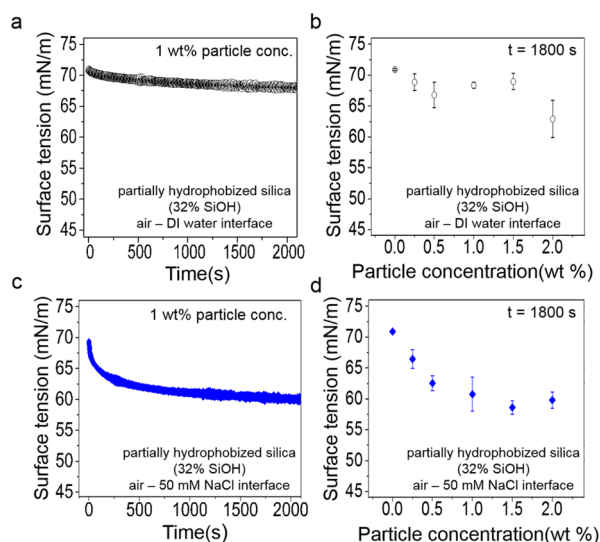


**Figure 2.** Interfacial activity of partially hydrophobized silica particles (32% SiOH) in the air–water interface. (a) Surface tension over time for 1 wt % particle dispersion. (b) Steady state surface tension obtained at  $t = 1800$  s for various particle concentrations. (c) Surface tension over time for 1 wt % particle dispersion in the presence of 50 mM NaCl. (d) Steady state surface tension obtained at  $t = 1800$  s for various concentrations of the surface-modified silica particles in the presence of 50 mM NaCl. Error bars represent the standard deviation of at least three replicate measurements.

investigated the steady state surface tension (taken at  $t = 1800$  s) of the aqueous dispersion with various concentrations of the same, partially hydrophobized silica particles ranging from 0 to 2 wt %. Figure 2b shows that the more hydrophobic silica particles slightly decrease the surface tension. To test whether the interfacial activity of these partially hydrophobized silica particles are limited by the electrostatic energy barrier, we measured the dynamic surface tension of a 1 wt % dispersion of these particles containing 50 mM NaCl. Figure 2c clearly shows that the surface tension decreases with time and reaches a lower steady state value than in the absence of salt, indicating partially hydrophobized silica particles display significant interfacial activity if the electrostatic interaction between the particle and the interface are screened by salt. We also studied the dependence of steady state surface tension on the particle concentration. Figure 2d shows that the long-term surface tension first decreases significantly with an increase in the particle concentration and then slightly increases with a further increase of particle concentration. We did not study the surface tension in the presence of even higher particle concentration (larger than 2 wt %) because the particle suspension becomes viscous at a higher particle concentration in the presence of salt.

In a control experiment with particle-free 1 M NaCl solution (at a concentration 40 times greater than its concentration used in the measurement), the surface tension as a function of time remains constant at 70.4 mN/m, showing the salt does not introduce surface-active impurities. Another battery of control experiments was carried out to confirm that the large reduction in surface tension was due to particle adsorption at the air–water interface and not due to the adsorption of water-soluble impurities originating with the silica particles or the residual acetone. The dynamic surface tension of the supernatant of a centrifuged dispersion of the hydrophobic silica particles was measured and shows close agreement with the surface tension of ultrapure DI water, which suggests that there are no significant surface-active contaminations or impurities in the particle suspension used in our study. The results of these control experiments verify that the change of the surface tension of the particle dispersion is caused by the particle adsorption and not by the salt or by impurities in the starting materials.

**Effect of Particles on the Tension of Hexadecane–Water Interfaces.** We also investigated the effect of particles on oil–water interfacial tension. The tension of a hexadecane–water interface was measured with silica particles dispersed in the water phase. Figure 3a shows the effective interfacial

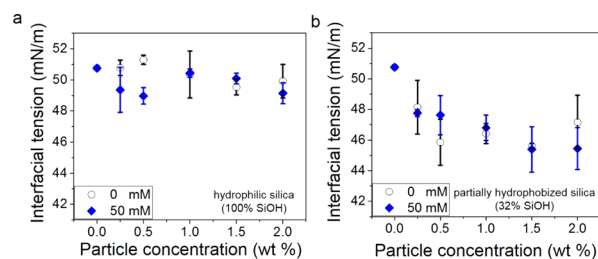


**Figure 3.** Interfacial activity of silica particles in the hexadecane oil–water interface. (a) Steady state hexadecane–water interfacial tension obtained at  $t = 1800$  s with hydrophilic silica particles (100% SiOH) at various particle concentrations. (b) Steady state hexadecane–water interfacial tension obtained at  $t = 1800$  s with hydrophobic silica particles (32% SiOH) at various particle concentrations. Error bars represent the standard deviation of at least three replicate measurements.

tensions (taken at  $t = 1800$  s) of the alkane with aqueous suspensions of the hydrophilic silica particles (100% SiOH) for particle concentrations ranging from 0 to 2 wt %. Figure 3a demonstrates that these hydrophilic silica particles have no strong effect on interfacial tension or only slightly decrease/increase the interfacial tension at the hexadecane–water interface. These results are expected from the weak affinity of very hydrophilic particles for the hexadecane–water interface. The poor long-term emulsion stability illustrated in Figure 4a also confirms the weak adsorption of hydrophilic silica particles at the hexadecane–water interface. Figure 3b shows the effective interfacial tension (at  $t = 1800$  s) of hexadecane with relatively hydrophobic silica particle (32% SiOH) suspensions in a particle concentration range from 0 to 2 wt %. Figure 3b demonstrates that the hydrophobically modified silica particles (32% SiOH) produce a larger reduction in interfacial tension than the very hydrophilic silica particles (100% SiOH). As shown in Figure 4b, the hydrophobically modified silica particles also mediate very good emulsion

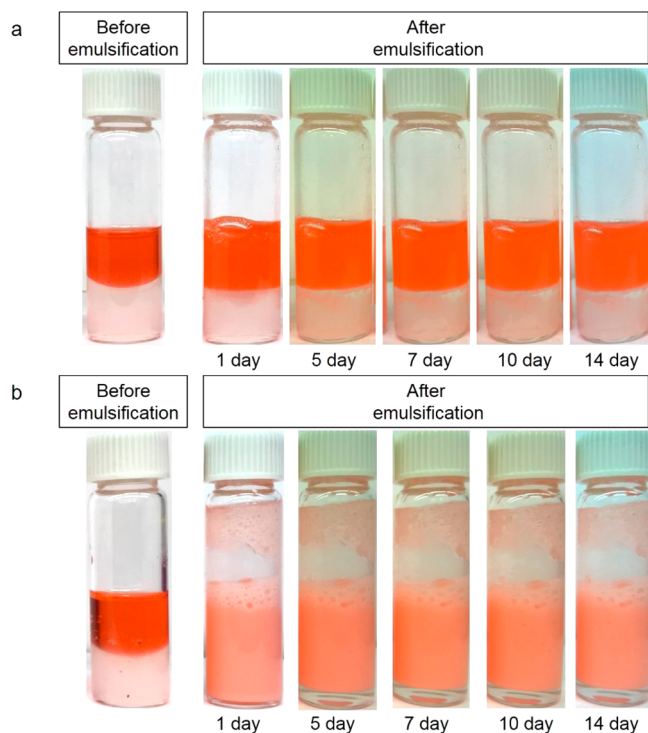


**Figure 4.** Long-term stability of hexadecane–water emulsions stabilized by silica particles. Aqueous 1 wt % dispersions of silica particles with an equal volume of hexadecane (stained with oil-soluble red dye Sudan III) were mixed using a rotor–stator homogenizer (IKA Ultra-Turrax T10) for 3 min at 11 000 rpm. (a) Unstable hexadecane–water emulsion prepared with hydrophilic silica particles (100% SiOH). (b) Stable hexadecane–water emulsion prepared with partially hydrophobized silica particles (32% SiOH).

stability, which further supports the notion that these particles adsorb strongly at the oil–water interface.

We further studied the influence of added salt on the reduction of hexadecane–water interfacial tension for dispersions of both particle types. Figures 3a and 3b show that the interfacial tension (after 1800 s) of hexadecane with the aqueous silica dispersions water is fairly insensitive to the presence of salt, suggesting that neither particle type experiences a significant barrier to adsorption at the oil–water interface. In the case of air–water interfaces, London–van der Waals interaction is repulsive, whereas for oil–water interfaces that interaction is attractive, which might contribute to the weaker adsorption barrier in the oil–water interface.

#### Theoretical Estimate of Effective Interfacial Tension.

The results presented above suggest that particles can reduce interfacial tensions if they do adsorb (overcoming any adsorption barrier) and have favorable wetting (a wetting angle not extremely far from  $90^\circ$  implies strong affinity to the interface). Next, we examine whether the observed particle effect on interfacial tension can be predicted theoretically. If particle–particle interactions are neglected (a common but potentially problematic approximation,<sup>32</sup> whose merit will be discussed further below), then the effective interfacial energy takes the form as shown by Du et al.:<sup>28</sup>

$$E' = \gamma_{ij}A + N_S \Delta E_{ad} \quad (2)$$

where  $\gamma_{ij}$  is the tension of bare interface between two fluids  $i$  and  $j$ ,  $A$  is the interfacial area,  $N_S$  is the number of adsorbed

particles in the interface, and  $\Delta E_{ad}$  is the energy benefit per particle adsorbed from the water phase, given by<sup>2,4,5</sup>

$$\Delta E_{ad} = -\pi R^2 \gamma_{ij} (1 - \cos \theta_{ijp})^2 \quad (3)$$

where  $R$  is the radius of the particle and  $\theta_{ijp}$  is the particle's equilibrium contact angle with the fluids  $i$  and  $j$  interface, measured through the water phase by convention.

From the thermodynamic definition of surface tension as the change in free energy per unit surface area, we can write an expression for the effective interfacial tension of the particle covered interface<sup>28</sup>

$$\gamma'_{ij} = (\partial E' / \partial A)_{N_S/A} = \gamma_{ij} + N_S \Delta E_{ad} / A \quad (4)$$

Combining eqs 3 and 4 yields the effective interfacial tension  $\gamma'_{ij}$  of the interface between two fluids  $i$  and  $j$  in the presence of particles as<sup>28</sup>

$$\gamma'_{ij} = \gamma_{ij} (1 - \phi (1 - \cos \theta_{ijp})^2) \quad (5)$$

where  $\phi = N_S \pi R^2 / A$  is the packing density (area fraction) of the particles adsorbed in the interface.

#### Comparison between Theoretically Predicted and Experimentally Measured Effective Interfacial Tension.

According to eq 5, an estimate of the effective interfacial tension in the presence of particles,  $\gamma'_{ij}$ , can be obtained from independently measured values of  $\gamma_{ij}$ ,  $\theta_{ijp}$ , and  $\phi$ . The interfacial tension  $\gamma_{ij}$  can be measured by a variety of methods, including axisymmetric drop shape analysis, as shown in our study. The three-phase particle contact angle ( $\theta_{ijp}$ ) can be determined using following methods:<sup>52</sup> indirect measurement (drop shape techniques, capillary rise methods, and surface pressure–area isotherms), direct measurement of multiple particles by the gel trapping method<sup>34</sup> or freeze–fracture shadow-casting cryo-scanning electron microscopy,<sup>35</sup> and direct measurements of single particles using digital holography.<sup>36</sup> As for the particle packing density, it can sometimes be inferred from direct microscopic observation; alternatively, it is possible to measure the average center-to-center distance between neighboring particles by use of in situ small-angle X-ray scattering.<sup>53</sup> An obvious question is how predictions for the effective interfacial tension  $\gamma'_{ij}$  in the presence of adsorbing particles from eq 5, with independently measured values of  $\gamma_{ij}$ ,  $\theta_{ijp}$ , and  $\phi$ , compare to direct measurements of  $\gamma'_{ij}$ . To address this question, we switched to a different system (TMPTMA–water interface), where the oil phase can be easily polymerized; thus, both the three-phase contact angle and the packing density are relatively easily to be measured. We examined the steady state interfacial tension of TMPTMA and water in the presence of 0.2 wt % EC particles. The effective interfacial tension of an EC particle-laden TMPTMA–water interface was obtained through eq 5 and independent measurements of  $\gamma_{ij}$ ,  $\theta_{ijp}$ , and  $\phi$ . A tension of  $19.2 \pm 0.1$  mN/m was obtained from axisymmetric drop shape analysis. The contact angle of EC particles in the TMPTMA–water interface is estimated as  $89.9 \pm 4.3^\circ$  from the contact angle of five TMPTMA drops under water on an EC-coated substrate (Figure 5a). TMPTMA is photopolymerizable, and recent studies indicate that the polymerization process does not change its interfacial properties.<sup>54–56</sup> Consequently, polymerizing a particle-laden TMPTMA droplet (Figure 5b) yields a solid version of the particle-decorated oil interface that facilitates the observation of the embedded particles. We examined two polymerized TMPTMA droplets by SEM and analyzed the area fraction of particles in 22 different locations

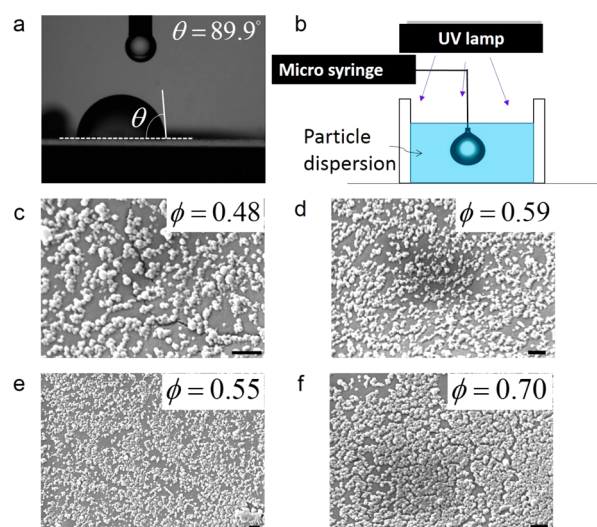


**Figure 5.** Measurements of contact angle and packing density of particles in fluid–fluid interfaces. (a) Image of a TMPTMA drop on a flat EC particle thin film placed inside the water medium. (b) Experimental setup for the measurement of the particle packing density in the TMPTMA–water interface. (c, d, e, f) SEM images of trapped EC particles at different locations on a polymerized TMPTMA droplet. Scale bars are 200 nm.

of the interfaces. Figures 5c–f are four representative SEM images of particles in different places of a polymerized TMPTMA droplet. From these images, we calculated the corresponding packing density of particles in the interface (as shown in Table 3). With the measured  $\gamma_{ij}$ ,  $\theta_{ijp}$ , and  $\phi$ , the calculated the effective interfacial tension of TMPTMA–water interface in the presence of 0.2 wt % EC particles is  $7.7 \pm 2.2$  mN/m (Figure 6 and Table 4). The large relative uncertainty of the calculated effective interfacial tension might be attributed to the challenge of obtaining accurate packing density and contact angle data for nanoparticles with a wide distribution of sizes and shapes in the fluid–fluid interfaces.

The effective interfacial tension of the TMPTMA–water interface in the presence of 0.2 wt % EC particles was also experimentally obtained by pendant drop tensiometry. The effective TMPTMA–water interfacial tension initially decreases and then reaches a plateau value of  $8.0 \pm 0.1$  mN/m, which agrees reasonably well the calculated effective interfacial tension of  $7.7 \pm 2.2$  based on eq 5. As a further test of eq 5, the adsorption of EC particles in the air–water interface was studied (Table 4). Since the packing density of EC particles was not accessible experimentally in this case, we increased the particle bulk concentration (up to 0.1 wt %) until no further decrease in surface tension (within 1800 s) could be achieved and assumed dense packing ( $\phi = 0.91$ ) of the air–water interface. The measured surface tension at this point is  $39.6 \pm 0.2$  mN/m, which agrees well with the calculated effective surface tension of  $39.2 \pm 1.7$  mN/m based on eq 5. In a study reported in 2010, Du et al.<sup>28</sup> measured the adsorption energy of

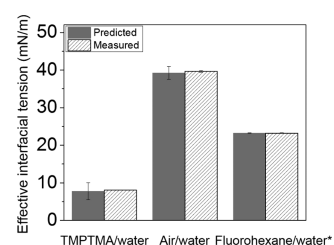


**Figure 6.** Comparison between theoretically predicted and experimentally measured effective interfacial tension. The fluorohexane/water result was based on ref 28.

polystyrene particles functionalized with amidine by monitoring the reduction of effective interfacial tension in the fluorohexane–water interface and assuming a closed-packed monolayer. From the contact angle, interfacial tension of the bare interface, and effective interfacial tension due to the adsorption of particles from this study, and assuming close packing of particles in the interface, eq 5 would predict an effective interfacial tension of  $23.2 \pm 0.10$  mN/m, in (unwarrantedly precise) agreement with the reported experimental result (Table 4). These comparisons suggest that eq 5 may provide a reasonable estimate of the effective interfacial tension with particles adsorbed in fluid–fluid interfaces.

**Packing Density Estimated from Dynamic Surface Tension Measurement.** The concentration of colloidal particles adsorbed to a fluid–fluid interface, which can be quantified as particle packing density or area fraction, plays a central role in many scientific problems and practical applications, for example, in the stabilization of foams and emulsions, food processing, and the colloidal assembly of functional microcapsules for pharmaceutical, agrochemical, or cosmetic formulations. Predicting the packing density of interfacially adsorbed particles can be difficult because it is strongly influenced in ways that are not well understood, by the interaction between particles adsorbed in the interface and the distributions of particle sizes and shapes. Similarly, it can be challenging to determine the packing density experimentally, especially for small particles or nanoparticles with a wide distribution of sizes or shapes. Clearly, an appropriate average may be more useful than a local value. Small-angle X-ray scattering (SAXS) and small-angle neutron scattering (SANS) provide such an average but require special instruments and sample preparation. Equation 5 implies that dynamic surface tension measurements ( $\gamma'_{ij}$  and  $\gamma_{ij}$ ), when combined with information about the particles' wetting properties ( $\theta_{ijp}$ ), provide a convenient and accurate way to assess the packing density of particles in fluid–fluid interfaces. Table 5 shows predicted packing densities obtained from eq 5 with measured tensions and contact angles. The predicted packing density of  $0.58 \pm 0.09$  for EC particles in the TMPTMA/water interface agrees well with the experimentally obtained local value of  $0.60 \pm 0.07$  (Table 5 and Figure 7). For the adsorption of EC particles in the air–water interface, the predicted packing density of  $0.90 \pm 0.05$  shows close agreement with the

**Table 3.** Packing Density and Contact Angle of EC Particles in the TMPTMA–Water Interfaces

|                |      |      |      |      |      |      |      |      |      |      |      | average | STD  |
|----------------|------|------|------|------|------|------|------|------|------|------|------|---------|------|
| $\Phi$         | 0.52 | 0.48 | 0.52 | 0.56 | 0.58 | 0.49 | 0.68 | 0.55 | 0.69 | 0.60 | 0.48 | 0.60    | 0.07 |
|                | 0.71 | 0.59 | 0.62 | 0.70 | 0.59 | 0.70 | 0.62 | 0.63 | 0.62 | 0.57 | 0.68 |         |      |
| $\theta$ (deg) | 86.2 | 85.4 | 89.5 | 95.6 | 92.6 |      |      |      |      |      |      | 89.9    | 4.3  |

**Table 4. Theoretically Predicted and Experimentally Measured Effective Interfacial Tension of Particles in Fluid–Fluid Interfaces**

| particles       | interfaces             | packing density | contact angle (deg) | interfacial tension (mN/m) | predicted effective interfacial tension (mN/m) | measured effective interfacial tension (mN/m) |
|-----------------|------------------------|-----------------|---------------------|----------------------------|--|---|
| ethyl cellulose | TMPTMA and water       | $0.6 \pm 0.07$  | $89.9 \pm 4.3$      | $19.2 \pm 0.1$             | $7.7 \pm 2.2$                                  | $8.0 \pm 0.1$                                 |
| ethyl cellulose | air and water          | 0.91            | $72.6 \pm 1.1$      | $70.9 \pm 0.2$             | $39.2 \pm 1.7$                                 | $39.6 \pm 0.2$                                |
| polystyrene     | fluorohexane and water | 0.91            | $36.9^a$            | $24.1 \pm 0.1$             | $23.2 \pm 0.1$                                 | $23.2 \pm 0.1$                                |

<sup>a</sup>The value here was inferred from ref 28, which reported the cosine of the contact angle as ranging from 0.8 to 1 and found the upper limit of the corresponding contact angle range,  $36.9^\circ$ , to be consistent with the independently determined energy of particle binding to the interface.

**Table 5. Theoretically Predicted and Experimentally Measured Packing Density of Particles in Fluid–Fluid Interfaces**

| particles       | interfaces             | contact angle (deg) | interfacial tension (mN/m) | effective interfacial tension (mN/m) | predicted packing density | measured/close packing density |
|-----------------|------------------------|---------------------|----------------------------|--------------------------------------|---------------------------|--------------------------------|
| ethyl cellulose | TMPTMA and water       | $89.9 \pm 4.3$      | $19.2 \pm 0.1$             | $8.0 \pm 0.1$                        | $0.58 \pm 0.09$           | $0.60 \pm 0.07$                |
| ethyl cellulose | air and water          | $72.6 \pm 1.1$      | $70.9 \pm 0.2$             | $39.6 \pm 0.2$                       | $0.90 \pm 0.05$           | 0.91                           |
| polystyrene     | fluorohexane and water | $36.9^a$            | $24.1 \pm 0.1$             | $23.2 \pm 0.1$                       | $0.93 \pm 0.14$           | 0.91                           |

<sup>a</sup>The value here was inferred from ref 28.

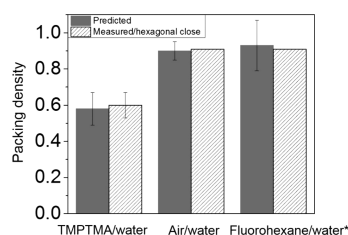


**Figure 7.** Comparison between theoretically predicted and experimentally measured packing density. The fluorohexane/water result was based on ref 28.

assumption of hexagonal close packing density of 0.91 (Table 5 and Figure 7). For the adsorption of polystyrene particles in the fluorohexane–water interface, although a large uncertainty for predicted packing density is observed, the predicted packing density of  $0.93 \pm 0.14$  is reasonably close to the hexagonal close packing density value of 0.91. Figure 7 suggests that the proposed method will be useful for studying the adsorption behavior of particles at fluid–fluid interfaces and will help in the directed assembly of particles for various applications.

**Final Considerations and Caveats.** Equation 5 relates the steady state interfacial tensions  $\gamma'$  and  $\gamma$ , which are comparatively easy to measure, with the interfacial particle packing fraction,  $\phi$ , and the particle contact angle,  $\theta$ , both of which can be difficult to determine experimentally.<sup>34,57,58</sup> To the extent that eq 5 can be trusted, it thus allows to infer any of the three parameters (tension, packing fraction, contact angle) from the experimental data for the remaining two. In particular, it could also be used to obtain contact angle information from interfacial tension and coverage. In practice, the uncertainty of the tension and coverage data will limit the usefulness of the approach: especially for low tension interfaces and particles with highly asymmetric wetting (contact angle far from  $90^\circ$ ) the tension drop due to particle adsorption will be small and typical uncertainties in the measured parameters translate into a large uncertainty for the inferred contact angle.

More fundamentally, it should surprise that eq 5 has any empirical merit in describing particle-saturated interfaces

because it does not explicitly include any particle–particle interactions but accounts for them only very crudely and indirectly through the finite packing fraction  $\phi$ . In this dubious approximation, the last particle that adsorbs to the already covered interface lowers the total interfacial energy by the exact same amount as the very first particle arriving at the pristine interface. Particles adsorbing at a later stage must interact with other adsorbed particles in a number of ways that are still not fully understood but can include long-range forces such as repulsive Coulombic and electrostatic dipole forces as well as attractive capillary forces arising from electrostatically induced interfacial deformations.<sup>59–61</sup> Recently, an attempt has been made to include some of these interactions in calculating the equilibrium coverage.<sup>47</sup> Apart from the daunting task of describing all the relevant in-plane interactions between adsorbed particles accurately, this approach relies on the premise that adsorption indeed achieves equilibrium coverage. In general, this may not be assumed. Repulsive interactions between particles approaching the interface and particles already adsorbed may set up an energy barrier that grows with increasing coverage and kinetically prevents further particle adsorption above a nonequilibrium threshold coverage. Finally, we would like to point out that while particle adsorption to fluid–fluid interfaces is obviously important for particle-stabilized emulsions and foams, the densest interfacial coverage in these systems is typically *not* achieved by particle adsorption, but through the coalescence of smaller, more sparsely covered droplets or bubbles.

## CONCLUSION

In summary, we have investigated the interfacial activity of silica nanoparticles for air–water and hexadecane–water interfaces using pendant drop tensiometry. Our measurements support the notion that simple, nonamphiphilic particles will reduce the interfacial tensions upon adsorption as long as they actually reach the interface and have favorable wetting; particles with contact angles near  $90^\circ$  affecting interfacial tension most strongly. A crude model was used to estimate the effective interfacial tensions of a particle-laden interface; its predictions

agree well with experimental results from pendant drop tensiometry. Finally, this study points at a simple way to estimate the average packing density of particles adsorbed to the fluid–fluid interface. Our findings and discussion may prove useful for understanding and directing nanoparticle assembly in liquid interfaces.

## ■ ASSOCIATED CONTENT

### 📄 Supporting Information

The Supporting Information is available free of charge on the ACS Publications website at DOI: [10.1021/acs.langmuir.7b00599](https://doi.org/10.1021/acs.langmuir.7b00599).

SEM images of silica and EC particles (Figure S1) (PDF)

## ■ AUTHOR INFORMATION

### Corresponding Authors

\*E-mail: [sven.behrens@chbe.gatech.edu](mailto:sven.behrens@chbe.gatech.edu).

\*E-mail: [carson.meredith@chbe.gatech.edu](mailto:carson.meredith@chbe.gatech.edu).

### ORCID

Ruiyang Zhao: [0000-0003-4930-1544](https://orcid.org/0000-0003-4930-1544)

J. Carson Meredith: [0000-0003-2519-5003](https://orcid.org/0000-0003-2519-5003)

### Notes

The authors declare no competing financial interest. Y.Z. and S.W. are co-first authors.

## ■ ACKNOWLEDGMENTS

We gratefully acknowledge financial support from the National Science Foundation (CBET-1134398, CBET-1160138), the Air Force Office of Scientific Research (Grant # FA9550-10-1-0555), and fellowship support for Y.Z. by the Renewable Bioproducts Institute (RBI), Georgia Institute of Technology. We also thank the generous donation of particles from Wacker-Chemie.

## ■ REFERENCES

- (1) Rosen, M. J.; Kunjappu, J. T. *Surfactants and Interfacial Phenomena*; Wiley: Hoboken, NJ, 2012.
- (2) Binks, B. P. Colloidal particles at liquid interfaces. *Phys. Chem. Chem. Phys.* **2007**, *9* (48), 6298–6299.
- (3) Wege, H. A.; Kim, S.; Paunov, V. N.; Zhong, Q. X.; Velev, O. D. Long-term stabilization of foams and emulsions with in-situ formed microparticles from hydrophobic cellulose. *Langmuir* **2008**, *24* (17), 9245–9253.
- (4) Pieranski, P. Two-dimensional interfacial colloidal crystals. *Phys. Rev. Lett.* **1980**, *45* (7), 569–572.
- (5) Binks, B. P.; Lumsdon, S. O. Influence of particle wettability on the type and stability of surfactant-free emulsions. *Langmuir* **2000**, *16* (23), 8622–8631.
- (6) Ramsden, W. Separation of solids in the surface-layers of solutions and suspensions (observations on surface-membranes, bubbles, emulsions, and mechanical coagulation).—preliminary account. *Proc. R. Soc. London* **1903**, *72*, 156–164.
- (7) Pickering, S. U. Emulsions. *J. Chem. Soc., Trans.* **1907**, *91*, 2001–2021.
- (8) Gonzenbach, U. T.; Studart, A. R.; Tervoort, E.; Gauckler, L. J. Ultrastable particle-stabilized foams. *Angew. Chem., Int. Ed.* **2006**, *45* (21), 3526–3530.
- (9) Levine, S.; Bowen, B. D.; Partridge, S. J. Stabilization of emulsions by fine particles 0.1. partitioning of particles between continuous phase and oil-water interface. *Colloids Surf.* **1989**, *38* (4), 325–343.
- (10) Aveyard, R.; Binks, B. P.; Clint, J. H. Emulsions stabilised solely by colloidal particles. *Adv. Colloid Interface Sci.* **2003**, *100*, 503–546.
- (11) Lee, D.; Weitz, D. A. Double emulsion-templated nanoparticle colloidosomes with selective permeability. *Adv. Mater.* **2008**, *20* (18), 3498–3503.
- (12) Cates, M. E.; Clegg, P. S. Bijels: a new class of soft materials. *Soft Matter* **2008**, *4* (11), 2132–2138.
- (13) Dinsmore, A. D.; Hsu, M. F.; Nikolaidis, M. G.; Marquez, M.; Bausch, A. R.; Weitz, D. A. Colloidosomes: selectively permeable capsules composed of colloidal particles. *Science* **2002**, *298* (5595), 1006–1009.
- (14) Aussillous, P.; Quere, D. Liquid marbles. *Nature* **2001**, *411* (6840), 924–927.
- (15) Dupin, D.; Armes, S. P.; Fujii, S. Stimulus-responsive liquid marbles. *J. Am. Chem. Soc.* **2009**, *131* (15), 5386–5387.
- (16) Zhang, Y.; Wu, J.; Wang, H.; Meredith, J. C.; Behrens, S. H. Stabilization of liquid foams through the synergistic action of particles and an immiscible liquid. *Angew. Chem.* **2014**, *126* (49), 13603–13607.
- (17) Zhang, Y.; Allen, M. C.; Zhao, R. Y.; Deheyn, D. D.; Behrens, S. H.; Meredith, J. C. Capillary foams: stabilization and functionalization of porous liquids and solids. *Langmuir* **2015**, *31* (9), 2669–2676.
- (18) Chevalier, Y.; Bolzinger, M. A. Emulsions stabilized with solid nanoparticles: Pickering emulsions. *Colloids Surf., A* **2013**, *439*, 23–34.
- (19) Vignati, E.; Piazza, R.; Lockhart, T. P. Pickering emulsions: interfacial tension, colloidal layer morphology, and trapped-particle motion. *Langmuir* **2003**, *19* (17), 6650–6656.
- (20) Fernandez-Rodriguez, M. A.; Ramos, J.; Isa, L.; Rodriguez-Valverde, M. A.; Cabrerizo-Vilchez, M. A.; Hidalgo-Alvarez, R. Interfacial activity and contact angle of homogeneous, functionalized, and Janus nanoparticles at the water/decane interface. *Langmuir* **2015**, *31* (32), 8818–8823.
- (21) Moghadam, T. F.; Azizian, S. Effect of ZnO nanoparticle and hexadecyltrimethylammonium bromide on the dynamic and equilibrium oil-water interfacial tension. *J. Phys. Chem. B* **2014**, *118* (6), 1527–1534.
- (22) Pichot, R.; Spyropoulos, F.; Norton, I. T. Competitive adsorption of surfactants and hydrophilic silica particles at the oil-water interface: Interfacial tension and contact angle studies. *J. Colloid Interface Sci.* **2012**, *377*, 396–405.
- (23) Drelich, A.; Gomez, F.; Clause, D.; Pezron, I. Evolution of water-in-oil emulsions stabilized with solid particles influence of added emulsifier. *Colloids Surf., A* **2010**, *365* (1–3), 171–177.
- (24) Manga, M. S.; Hunter, T. N.; Cayre, O. J.; York, D. W.; Reichert, M. D.; Anna, S. L.; Walker, L. M.; Williams, R. A.; Biggs, S. R. Measurements of sub-micron particle adsorption and particle film elasticity at oil-water interfaces. *Langmuir* **2016**, *32* (17), 4125–4133.
- (25) Dong, L. C.; Johnson, D. Surface tension of charge-stabilized colloidal suspensions at the water-air interface. *Langmuir* **2003**, *19* (24), 10205–10209.
- (26) Bizmark, N.; Ioannidis, M. A.; Henneke, D. E. Irreversible adsorption-driven assembly of nanoparticles at fluid interfaces revealed by a dynamic surface tension probe. *Langmuir* **2014**, *30* (3), 710–717.
- (27) Stocco, A.; Drenckhan, W.; Rio, E.; Langevin, D.; Binks, B. P. Particle-stabilised foams: an interfacial study. *Soft Matter* **2009**, *5* (11), 2215–2222.
- (28) Du, K.; Glogowski, E.; Emrick, T.; Russell, T. P.; Dinsmore, A. D. Adsorption Energy of Nano- and Microparticles at Liquid-Liquid Interfaces. *Langmuir* **2010**, *26* (15), 12518–12522.
- (29) Powell, K. C.; Chauhan, A. Interfacial tension and surface elasticity of carbon black (CB) covered oil-water interface. *Langmuir* **2014**, *30* (41), 12287–12296.
- (30) Hua, X. Q.; Bevan, M. A.; Frechette, J. Reversible partitioning of nanoparticles at an oil-water interface. *Langmuir* **2016**, *32* (44), 11341–11352.
- (31) Zhang, Y.; Shitta, A.; Meredith, J. C.; Behrens, S. H. Bubble meets droplet: particle-assisted reconfiguration of wetting morphologies in colloidal multiphase systems. *Small* **2016**, *12* (24), 3309–3319.
- (32) Fan, H.; Striolo, A. Nanoparticle effects on the water-oil interfacial tension. *Phys. Rev. E* **2012**, *86* (5). [10.1103/PhysRevE.86.051610](https://doi.org/10.1103/PhysRevE.86.051610).

- (33) Worthen, A. J.; Bagaria, H. G.; Chen, Y. S.; Bryant, S. L.; Huh, C.; Johnston, K. P. Nanoparticle-stabilized carbon dioxide-in-water foams with fine texture. *J. Colloid Interface Sci.* **2013**, *391*, 142–151.
- (34) Paunov, V. N. Novel method for determining the three-phase contact angle of colloid particles adsorbed at air-water and oil-water interfaces. *Langmuir* **2003**, *19* (19), 7970–7976.
- (35) Isa, L.; Lucas, F.; Wepf, R.; Reimhult, E. Measuring single-nanoparticle wetting properties by freeze-fracture shadow-casting cryo-scanning electron microscopy. *Nat. Commun.* **2011**, *2*, 438.
- (36) Kaz, D. M.; McGorty, R.; Mani, M.; Brenner, M. P.; Manoharan, V. N. Physical ageing of the contact line on colloidal particles at liquid interfaces. *Nat. Mater.* **2011**, *11* (2), 138–142.
- (37) Kostakis, T.; Ettelaie, R.; Murray, B. S. Effect of high salt concentrations on the stabilization of bubbles by silica particles. *Langmuir* **2006**, *22* (3), 1273–1280.
- (38) Jin, H. J.; Zhou, W. Z.; Cao, J.; Stoyanov, S. D.; Blijdenstein, T. B. J.; de Groot, P. W. N.; Arnaudov, L. N.; Pelan, E. G. Super stable foams stabilized by colloidal ethyl cellulose particles. *Soft Matter* **2012**, *8* (7), 2194–2205.
- (39) Behrens, S. H.; Grier, D. G. The charge of glass and silica surfaces. *J. Chem. Phys.* **2001**, *115* (14), 6716–6721.
- (40) Bueno-Tokunaga, A.; Perez-Garibay, R.; Martinez-Carrillo, D. Zeta potential of air bubbles conditioned with typical froth flotation reagents. *Int. J. Miner. Process.* **2015**, *140*, 50–57.
- (41) Elmahdy, A. M.; Mirnezami, M.; Finch, J. A. Zeta potential of air bubbles in the presence of frothers. *Int. J. Miner. Process.* **2008**, *89* (1–4), 40–43.
- (42) Oliveira, C.; Rubio, J. Zeta potential of single and polymer-coated microbubbles using an adapted microelectrophoresis technique. *Int. J. Miner. Process.* **2011**, *98* (1–2), 118–123.
- (43) Song, K. B.; Damodaran, S. Influence of electrostatic forces on the adsorption of succinylated beta-lactoglobulin at the air-water interface. *Langmuir* **1991**, *7* (11), 2737–2742.
- (44) Damodaran, S.; Xu, S. Q. The role of electrostatic forces in anomalous adsorption behavior of phosvitin at the air/water interface. *J. Colloid Interface Sci.* **1996**, *178* (2), 426–435.
- (45) Wang, H.; Singh, V.; Behrens, S. H. Image charge effects on the formation of pickering emulsions. *J. Phys. Chem. Lett.* **2012**, *3* (20), 2986–2990.
- (46) Kutuzov, S.; He, J.; Tangirala, R.; Emrick, T.; Russell, T. P.; Böker, A. On the kinetics of nanoparticle self-assembly at liquid/liquid interfaces. *Phys. Chem. Chem. Phys.* **2007**, *9* (48), 6351–6358.
- (47) Dugyala, V. R.; Muthukuru, J. S.; Mani, E.; Basavaraj, M. G. Role of electrostatic interactions in the adsorption kinetics of nanoparticles at fluid-fluid interfaces. *Phys. Chem. Chem. Phys.* **2016**, *18* (7), 5499–5508.
- (48) Tabor, R. F.; Manica, R.; Chan, D. Y. C.; Grieser, F.; Dagastine, R. R. Repulsive van der Waals forces in soft matter: why bubbles do not stick to walls. *Phys. Rev. Lett.* **2011**, *106* (6), 064501.
- (49) Binks, B. P.; Murakami, R. Phase inversion of particle-stabilized materials from foams to dry water. *Nat. Mater.* **2006**, *5* (11), 865–869.
- (50) Okubo, T. Surface tension of structured colloidal suspensions of polystyrene and silica spheres at the air-water interface. *J. Colloid Interface Sci.* **1995**, *171* (1), 55–62.
- (51) Binks, B. P.; Horozov, T. S. Aqueous foams stabilized solely by silica nanoparticles. *Angew. Chem., Int. Ed.* **2005**, *44* (24), 3722–3725.
- (52) Snoeyink, C.; Barman, S.; Christopher, G. F. Contact angle distribution of particles at fluid interfaces. *Langmuir* **2015**, *31* (3), 891–897.
- (53) Lin, Y.; Böker, A.; Skaff, H.; Cookson, D.; Dinsmore, A. D.; Emrick, T.; Russell, T. P. Nanoparticle assembly at fluid interfaces: structure and dynamics. *Langmuir* **2005**, *21* (1), 191–194.
- (54) Xu, H.; Goedel, W. A. Particle-assisted wetting. *Langmuir* **2003**, *19* (12), 4950–4952.
- (55) Ding, A. L. PhD Dissertation. Chemnitz University of Technology, 2007.
- (56) Ding, A. L.; Goedel, W. A. Experimental investigation of particle-assisted wetting. *J. Am. Chem. Soc.* **2006**, *128* (15), 4930–4931.
- (57) Li, Z.; Giese, R. F.; Vanoss, C. J.; Yvon, J.; Cases, J. The surface thermodynamic properties of talc treated with octadecylamine. *J. Colloid Interface Sci.* **1993**, *156* (2), 279–284.
- (58) Aveyard, R.; Clint, J. H.; Nees, D.; Paunov, V. N. Compression and structure of monolayers of charged latex particles at air/water and octane/water interfaces. *Langmuir* **2000**, *16* (4), 1969–1979.
- (59) Wurger, A.; Foret, L. Capillary attraction of colloidal particles at an aqueous interface. *J. Phys. Chem. B* **2005**, *109* (34), 16435–8.
- (60) Boneva, M. P.; Danov, K. D.; Christov, N. C.; Kralchevsky, P. A. Attraction between Particles at a Liquid Interface Due to the Interplay of Gravity- and Electric-Field-Induced Interfacial Deformations. *Langmuir* **2009**, *25* (16), 9129–9139.
- (61) Dominguez, A.; Oettel, M.; Dietrich, S. Dynamics of colloidal particles with capillary interactions. *Phys. Rev. E* **2010**, *82* (1), 18.